

Buffer-gas-induced collision shift for the $^{88}\text{Sr } ^1S_0\text{-}^3P_1$ clock transition

Nobuyasu Shiga,¹ Ying Li,¹ Hiroyuki Ito,¹ Shigeo Nagano,¹ Tetsuya Ido,^{1,2,*} Katarzyna Bielska,³ Ryszard S. Trawiński,³ and Roman Ciuryło³

¹National Institute of Information and Communications Technology, Koganei, Tokyo 184-8795, Japan

²CREST, Japan Science and Technology Agency, Chiyoda-ku, Tokyo 102-0075, Japan

³Instytut Fizyki, Uniwersytet Mikołaja Kopernika, ul. Grudziadzka 5/7, 87-100 Toruń, Poland

(Received 3 July 2009; published 4 September 2009)

Precision saturation spectroscopy of the $^{88}\text{Sr } ^1S_0\text{-}^3P_1$ is performed in a vapor cell filled with various rare gases including He, Ne, Ar, and Xe. By continuously calibrating the absolute frequency of the probe laser, buffer-gas-induced collision shifts of $\sim\text{kHz}$ are detected with gas pressure of 1–20 mTorr. Helium gave the largest fractional shift of $1.6 \times 10^{-9} \text{ Torr}^{-1}$. Comparing with a simple impact calculation and a Doppler-limited experiment of Holtgrave and Wolf [J. C. Holtgrave and P. J. Wolf, Phys. Rev. A **72**, 012711 (2005)], our results show larger broadening and smaller shifting coefficient, indicating effective atomic loss due to velocity-changing collisions. The applicability of the result to the $^1S_0\text{-}^3P_0$ optical lattice clock transition is also discussed.

DOI: 10.1103/PhysRevA.80.030501

PACS number(s): 32.70.Jz, 32.30.Jc, 34.10.+x

From the beginning of laser spectroscopy, frequency shifts and broadening caused by background gas collisions have been investigated both experimentally and theoretically [1]. The spin-forbidden transitions $^1S_0\text{-}^3P_1$ from the ground states of bosonic two-outer-electron atoms have been major testing grounds due to their fairly narrow natural linewidths and level simplicity free from hyperfine structure. Experiments were done for Ca [2], Sr [2–4], Cd [5,6], Hg [7,8], and Yb [9] with perturber pressures of $10^0\text{--}10^2$ Torr. In these experiments, shifts and broadenings exceed 10 MHz, and higher-order effects such as collision time asymmetry or speed dependence of collisional broadening and shifting were observed [10,11]. Performing the spectroscopy in lower pressure provides the accurate measurement of the linear collision shift and broadening.

The research of the atomic clock is one area that would benefit from the accurate measurement of the linear collision shift. The latest progress of optical clocks is so rapid that a fractional accuracy of $\sim 10^{-17}$ was demonstrated with single-ion systems [12] and $\sim 10^{-16}$ with Sr lattice clock [13]. This remarkable precision, on the other hand, requires us to consider various systematic shifts which have been so far ignored. Collision shifts induced by background gas (BG) [14] may ultimately limit the accuracy in this unprecedented level. However, the characterization of BG-induced collision shifts is difficult in real clocks because the deliberate injection of buffer gas for the shifting of atomic resonance normally causes loss of atoms, limiting the coherence time needed to evaluate subtle BG induced shifts.

In this Rapid Communication, buffer-gas-induced collision shifts for the $^{88}\text{Sr } ^1S_0\text{-}^3P_1$ transition is reported based on precision saturation absorption spectroscopy with the phase-modulation technique [15,16]. Continuously monitoring the probe laser frequency using a frequency comb referenced to international atomic time (TAI), we compared the resonance frequency with the true atomic resonance measured with ul-

tracold atoms [17]. The detected background-gas-induced collision shift was $\sim\text{kHz}$, which is, to the best of our knowledge, the finest definitive measurement of optical frequency shifts induced by foreign-gas collisions.

The $(5s^2)^1S_0\text{-}(5s5p)^3P_1$ transition at $\lambda=689 \text{ nm}$ ($c/\lambda=434.829 \text{ THz}$ [18]) has a natural linewidth $\gamma=2\pi \times 7.4 \text{ kHz}$, which corresponds to the saturation intensity $I_s=2\pi^2\hbar c\gamma/3\lambda^3=2.9 \mu\text{W}/\text{cm}^2$, where c and $2\pi\hbar$ is the speed of light and the Planck constant, respectively. The experimental setup of our saturated absorption spectroscopy is shown in Fig. 1. The spectral width of an extended cavity diode laser is reduced to less than 500 Hz by locking the laser frequency to a cavity with a basic Pound-Drever-Hall (PDH) method [19]. The modulation index is 0.17 and the frequency is 21.7 MHz. This modulation is used for the saturation absorption spectroscopy as well. Strontium is contained in a heat pipe oven [20] with Brewster window plates separated by 75 cm. The typical temperature of the pipe is 728 K. The two ends of the active area (20 cm length) are water cooled, so that the strontium is not deposited on the windows. The buffer gas is introduced from one end of the

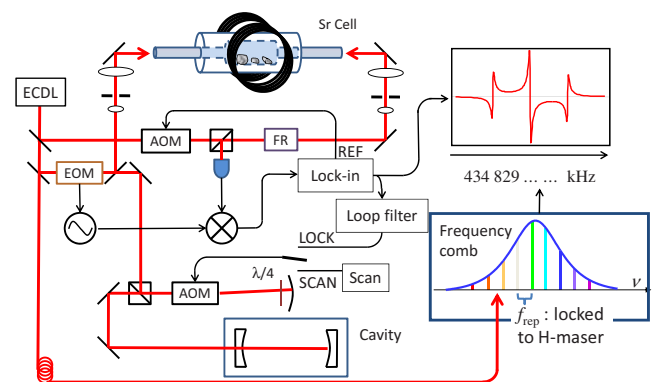


FIG. 1. (Color online) Experimental configuration of the precision saturated absorption spectroscopy. ECDL: extended cavity diode laser; FR: Faraday rotator; EOM: Electro-optic modulator; AOM: acousto-optic modulator.

*Corresponding author; ido@nict.go.jp

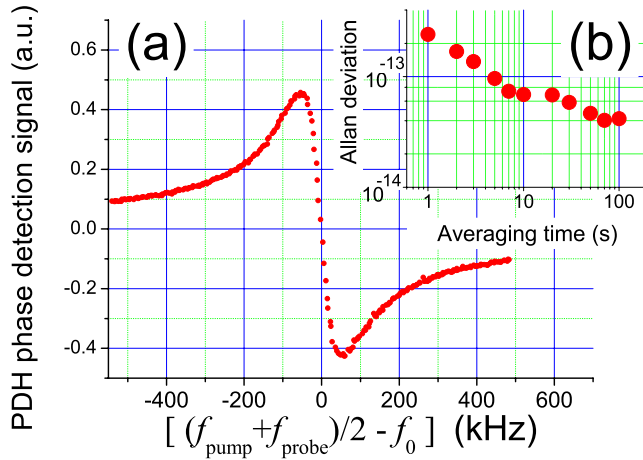


FIG. 2. (Color online) (a) Dispersion signal of phase modulation spectroscopy. The offset frequency of $f_0=434\,829\,121\,312$ kHz is the true atomic resonance measured in [17]. (b) Modified Allan standard deviation of the 689 nm laser frequency tightly locked to the resonance signal obtained by the saturation spectroscopy.

pipe after flushing the pipe several times, and Pirani gauges are installed at both ends for the confirmation of uniform pressures in the tube. The magnetic sublevels are well defined by a bias magnetic field of 3 G produced by a Helmholtz coil pair. Pump and probe beams of the saturation spectroscopy have the same linear polarization, which excites the π transition of $\Delta m_J=0$. Pinholes are placed in both arms to overlap the pump and the probe beams. The peak intensity and the $1/e^2$ radius of the pump beam (probe beam) are $270\ \mu\text{W}/\text{cm}^2$ and 4.2 mm ($50\ \mu\text{W}/\text{cm}^2$ and 3.3 mm), respectively. After interacting with Sr vapor, the polarization of the probe beam is rotated 90° and coupled out by a polarization beam splitter. The pump beam is frequency shifted by 80 MHz from the probe beam in order to avoid dc noise caused by the interference between the two beams. In addition, the pump beam is chopped with a frequency of 5 kHz to extract the saturation signal induced by the pump beam. The absolute frequency of the laser is always monitored by a frequency comb referenced to TAI.

A sample of PDH phase detection signal with helium buffer gas of 4×10^{-4} Torr is shown in Fig. 2(a). The absolute frequency of the probe laser is expressed as a differential frequency $(f_{\text{pump}} + f_{\text{probe}})/2 - f_0$, where f_{pump} and f_{probe} are the pump and the probe laser frequencies, respectively, and the true atomic resonance f_0 is the frequency precisely measured in [17] from ballistically expanding ultracold atoms. The full width half maximum is nonlinear fitted to be 107 kHz, which agrees with saturation broadening (80 kHz) and transit time broadening (31 kHz) expected from the beam intensity and diameter. This dispersion shape works as an error signal to lock the laser. The stability of this Sr vapor cell clock is shown in Fig. 2(b) as modified Allan deviation against a hydrogen maser. The bottom of the instability is 4×10^{-14} at 100 s. The stability is limited by fluctuations of buffer gas and vapor pressure or pump beam intensity that changes the light-pressure-induced line-shape asymmetry [21].

We measured the pressure dependence of the background-gas-induced broadening and shift for various background gases. The buffer gases are rare gases, namely, helium, neon, argon, and xenon. The attempts to fill with nitrogen failed since the gas was quickly adsorbed by solid strontium. The broadening is determined from the dispersion curve as in Fig. 2(a). Locking the laser frequency to the zero crossing of dispersion curve, the resonance is determined by a frequency comb that is referenced to TAI. We determined the slope of the collisional broadening and the frequency shift as a function of the buffer gas pressure by doing a least-squares fit, and the result is summarized in Table I.

The frequency shift data are summarized in Fig. 3. The experimental condition described above has resulted in a residual offset of -4 kHz from the true atomic resonance. Part of the reason is a shift caused by homonuclear two-body collisions. By changing the temperature of the heat pipe oven, we measured the Sr-Sr collision shift coefficient to be -1.3×10^{-10} Hz cm^3 [22]. This effect causes a shift of -1 kHz for the condition of Fig. 3. We suspect that the most probable reason for the remaining -3 kHz is residual Doppler shifts. The spatial filters in the two arms still permit a mutual beam tilt of $\theta=62\ \mu\text{rad}$. In the case that atoms are directed as in an atomic beam, this tilt causes Doppler shift

TABLE I. The comparison of our experimental pressure broadening and shifting coefficients with those calculated in the impact approximation, as well as with experimental results obtained by Holtgrave and Wolf [4] in the Doppler limited regime and obtained by Tino *et al.* [3] in the Doppler free regime. All data are given in MHz/Torr and the one standard deviation uncertainties are given in parentheses.

Perturber	Doppler limited				Doppler free			
	Experiment Holtgrave and Wolf		Impact calculation ($T=660$ K)		Experiment This work		Impact calculation ($T=728$ K)	
	Γ/p	Δ/p	Γ/p	Δ/p	Γ/p	Δ/p	Γ/p	Δ/p
He	3.79(17)	+1.23(6)	3.89	+0.68	8.67(10)	+0.68(8)	3.68	+0.66
Ne	2.60(13)	-0.64(4)	1.17	-0.31	3.76(5)	-0.06(3)	1.10	-0.28
Ar	2.45(04)	-1.45(4)	3.30	-1.54	4.76(8)	-0.22(2)	3.05	-1.47
Xe	3.44(23)	-1.51(3)	3.35	-1.36	5.5(5) ^a	-0.12(1)	3.17	-1.33

^aResult obtained by Tino *et al.* [3].

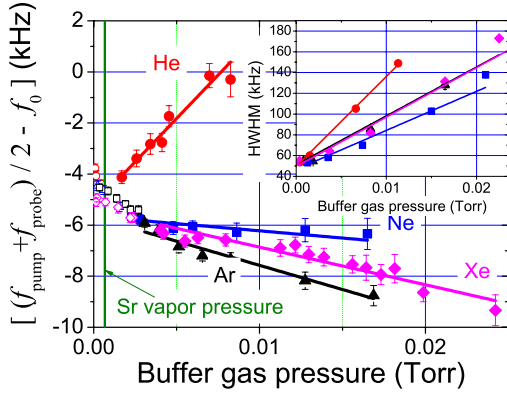


FIG. 3. (Color online) Shifts of the resonance frequency induced by various kinds of buffer gas. The corner of the slope around 3 mTorr is attributed to the inhomogeneous pressure distribution in the cell, which occurs due to insufficient buffer gas pressure relative to strontium vapor. Inset is the broadening of the Doppler-free atomic resonance.

of $k_L v_m \sin(\theta/2) = 15$ kHz maximum, where k_L is the wave number of the light, $v_m = \sqrt{2k_B T/m} = 371$ m/s is the most probable speed of Sr atoms at gas temperature $T = 728$ K, m is the Sr mass, and k_B is the Boltzmann constant. Our spectroscopy is ideally performed with an isotropic velocity distribution of atoms. However, a slightly biased velocity distribution may be produced in the oven due to an inhomogeneous temperature distribution of the pipe. Since the beam passes above bulk solid strontium, the distribution could be biased upward.

Only the collisions with He show a positive shift coefficient, whereas Ne, Ar, and Xe show negative coefficients. The open symbols at lower pressures are excluded from the fitting since the vapor pressure of strontium is not small enough comparing with the buffer gas pressure. Even slightly above the vapor pressure, the buffer gas pressure was not spatially uniform at pressures below 3×10^{-3} Torr. We added the buffer gas from one side, and the spatial gradient of the gas pressure was observed by Pirani gauges placed at the both ends.

The collisional width Γ [half-width at half maximum (HWHM)] and shift Δ in the impact approximation are proportional to the density of perturbers N and are given by the well-known expression [1,23]

$$\Gamma + i\Delta = N \int d^3\vec{v}_r f_\mu(\vec{v}_r) v_r \int_0^\infty d\rho \rho \{1 - \langle S_{if} S_{ff}^{-1} \rangle_{Av}\}, \quad (1)$$

where $f_\mu(\vec{v}_r)$ is the Maxwellian distribution of relative velocities \vec{v}_r of colliding absorber and perturber having a reduced mass μ and ρ is the impact parameter. In this work we report results obtained in the mean speed approximation in which calculations are done just for the mean relative speed $\bar{v} = \sqrt{8k_B T/(\pi\mu)}$ of colliding atoms. For the intercombination transition $^1S_0 - ^3P_1$, in the adiabatic approximation the angular average of scattering matrix elements in the initial and the final states $\langle S_{if} S_{ff}^{-1} \rangle_{Av} = \frac{1}{3} e^{-i\eta_{A-X}} + \frac{2}{3} e^{-i\eta_{B-X}}$ can be expressed in terms of phase shifts η_{A-X} and η_{B-X} induced by the quasimolecular transitions $A^3O^+ - X^1O^+$ and $B^31 - X^1O^+$,

respectively [11,24]. These phase shifts are integrals $\eta = \int_{-\infty}^{+\infty} dt \Delta V(r(t))/\hbar$ of the excited and the ground electronic state potentials differences $V(A^3O^+) - V(X^1O^+)$ and $V(B^31) - V(X^1O^+)$ for Sr-Rg (He, Ne, Ar, Xe) systems. For simplicity we assumed straight line trajectories with the interatomic separation $r(t) = \sqrt{\rho^2 + v_r^2 t^2}$.

The interaction potentials are approximated here by a modified Lennard-Jones formula $V(r) = C_{12}/r^{12} + C_8/r^8 + C_6/r^6$. Following Hindmarsh *et al.* [25] C_{12} coefficients are estimated using Hindmarsh radii $r_H(\text{Rg})$ for rare gases Rg [26] and $r_H(\text{Sr})$ for Sr. The Hindmarsh radii $r_H(\text{Sr})$ have been estimated using the charge densities calculated by Mitroy and Zhang [27]. They were found to be $9.4773a_0$ and $10.8801a_0$ in the ground 1S_0 and in the excited $^3P_{0,1,2}$ electronic states of Sr atom, respectively. The atomic unit of length is $a_0 \approx 0.05292$ nm. The dispersion coefficients C_6 and C_8 for Sr-Rg were also calculated by Mitroy and Zhang [27]. The dispersion coefficient given for excited states $^3\Sigma^+$ and $^3\Pi$ were converted to appropriate coefficients for states A^3O^+ and B^31 using the following asymptotic relations: $C_6(A^3O^+) = C_6(^3\Pi)$ and $C_6(B^31) = \frac{1}{2} C_6(^3\Sigma^+) + \frac{1}{2} C_6(^3\Pi)$. The term C_8/r^8 included in our calculations allows for a better description of the interaction anisotropy in the excited state of Sr. We note that the addition of the C_8/r^8 and C_{10}/r^{10} terms to the interaction model changes the calculated broadening about a factor of 2. The change can be even bigger in the case of the shift and for Ne it can lead to a change in its sign. We also verified that if the thermal average is neglected, the resulting error is less than 5%. The positive collisional shift observed for He is caused by the dominating influence of the repulsive interaction C_{12}/r^{12} on the collisional broadening and shifting.

Table I shows the comparison of the pressure broadening and shifting coefficients measured in this work with those calculated in the impact approximation [Eq. (1)] and experimental results obtained by other authors. There is only one full set of data for rare-gas pressure broadening and shifting of strontium intercombination line reported by Holtgrave and Wolf [4]. Results of Ref. [4] were obtained in the Doppler-limited regime at a temperature of 660(47) K, where the magnitude of the broadening and shifts exceed 100 MHz. Note that collisional broadening cross section determined by Holtgrave and Wolf agree very well with those obtained by Crane *et al.* [2] for Ar and differ by 23% from those for Ne. In Ref. [2] also the Doppler-limited spectroscopical method was used. It is clear that our results do not agree with those obtained using Doppler-limited spectroscopy [2,4]. On the other hand our results agree well with those determined by Tino *et al.* [3] for Ar in the Doppler-free regime (see Table I).

The comparison of calculated results seems to give a bit better agreement with results obtained in the Doppler-limited case. Clearly Doppler-free results are characterized by bigger collision broadening coefficients and smaller magnitude of collision-shifting coefficients than those obtained from the Doppler-limited case. This can be attributed to velocity-changing collisions [28], which change the absorber velocity significantly enough to push away the absorber from the condition of Doppler-free resonance. Therefore, such events of collisions which can cause large frequency shifts in the

Doppler-limited regime would not contribute to the signal in the Doppler-free case. Being a loss mechanism, it will lead to broadening but not to shifting of the line. This effect needs further theoretical and experimental investigations. Moreover, in these investigations it would be very useful to carry out proper close-coupling broadening and shifting calculations [29] based on *ab initio* potentials.

The cold strontium system is currently studied extensively in many national standards institutes due to its application to optical lattice clocks [30]. For the clock transition 1S_0 - 3P_0 , the interaction of the ground-state rare-gas atom with the excited clock atom at 3P_0 state is described by just one potential curve denoted as $^30^-$ approaching dissociation limit. The dispersion coefficient describing this interaction fulfills the relation $C_6(^30^-) = C_6(^3\Pi)$ and with a good approximation is equal to $C_6(A\ ^30^+)$ investigated here. Moreover, in the case of collisions of clock atoms with background gas atoms, the velocity-changing collisions will also play a crucial role leading to relatively large collisional broadening and small collisional shifting. Therefore, results obtained here as well

as the discrepancy of the shift coefficients depending on Doppler-free or -limited system should help to correctly estimate the impact of residual-gas-induced collision shift on optical atomic clocks. The values of fractional shift coefficients $< 2 \times 10^{-9}$ Torr $^{-1}$ obtained here can be treated as an upper limit for shifts caused by the residual gas in optical lattice clocks. Since the state-of-the-art optical lattice clocks are currently operated in a vacuum pressure of $\sim 10^{-9}$ Torr, the shifts due to the residual gases would not be an issue until the accuracy of the clock reaches the $\sim 10^{-18}$ level.

We thank J. Mitroy and J.-Y. Zhang for their calculation of various C_n numbers for strontium. We acknowledge the fruitful comment and experimental help from W. Itano, M. Hosokawa, M. Kajita, A. Yamaguchi, M. Koide, and H. Ishijima. The theoretical part of this work was supported by the Polish MNISW (Project No. N N202 1489 33) as a part of the program of the National Laboratory FAMO in Toruń, Poland.

-
- [1] N. Allard and J. Kielkopf, *Rev. Mod. Phys.* **54**, 1103 (1982); J. Szudy and W. E. Baylis, *Phys. Rep.* **266**, 127 (1996).
- [2] J. K. Crane, M. J. Shaw, and R. W. Presta, *Phys. Rev. A* **49**, 1666 (1994).
- [3] G. M. Tino *et al.*, *Appl. Phys. B: Lasers Opt.* **55**, 397 (1992).
- [4] J. C. Holtgrave and P. J. Wolf, *Phys. Rev. A* **72**, 012711 (2005).
- [5] K. J. Dietz *et al.*, *J. Phys. B* **13**, 2749 (1980).
- [6] A. Bielski *et al.*, *Acta Phys. Pol. B* **33**, 2267 (2002); R. S. Trawinski, R. Ciurylo, and J. Szudy, *Phys. Rev. A* **74**, 022716 (2006).
- [7] J. P. Jacobs and R. B. Warrington, *Phys. Rev. A* **68**, 032722 (2003).
- [8] T. N. Anderson *et al.*, *Appl. Phys. B: Lasers Opt.* **87**, 341 (2007).
- [9] D. F. Kimball *et al.*, *Phys. Rev. A* **60**, 1103 (1999).
- [10] I. Shannon *et al.*, *J. Phys. B* **19**, 1409 (1986).
- [11] A. Bielski *et al.*, *Phys. Rev. A* **62**, 032511 (2000).
- [12] T. Rosenband *et al.*, *Science* **319**, 1808 (2008).
- [13] A. D. Ludlow *et al.*, *Science* **319**, 1805 (2008).
- [14] Y. Sortais *et al.*, *Phys. Rev. Lett.* **85**, 3117 (2000).
- [15] J. L. Hall *et al.*, *Appl. Phys. Lett.* **39**, 680 (1981).
- [16] G. C. Bjorklund *et al.*, *Appl. Phys. B: Lasers Opt.* **32**, 145 (1983).
- [17] T. Ido *et al.*, *Phys. Rev. Lett.* **94**, 153001 (2005).
- [18] G. Ferrari *et al.*, *Phys. Rev. Lett.* **91**, 243002 (2003).
- [19] R. W. P. Drever *et al.*, *Appl. Phys. B: Lasers Opt.* **31**, 97 (1983).
- [20] C. R. Vidal and J. Cooper, *J. Appl. Phys.* **40**, 3370 (1969).
- [21] R. Grimm and J. Mlynek, *Phys. Rev. Lett.* **63**, 232 (1989); R. Grimm and J. Mlynek, *Phys. Rev. A* **42**, 2890 (1990).
- [22] This coefficient is ten times less than that measured with cold atoms [17].
- [23] M. Baranger, *Phys. Rev.* **111**, 494 (1958).
- [24] A. Bielski *et al.*, *Acta Phys. Pol. A* **90**, 1155 (1996); **105**, 217 (2004).
- [25] W. R. Hindmarsh *et al.*, *Proc. R. Soc. London, Ser. A* **197**, 296 (1967).
- [26] A. Bielski and J. Wasilewski, *Z. Naturforsch [C]* **35a**, 1112 (1980).
- [27] J. Mitroy and J.-Y. Zhang, *J. Chem. Phys.* **128**, 134305 (2008); (private communication).
- [28] P. R. Berman, P. F. Liao, and J. E. Bjorkholm, *Phys. Rev. A* **20**, 2389 (1979).
- [29] P. S. Julienne and F. H. Mies, *Phys. Rev. A* **34**, 3792 (1986); P. J. Leo *et al.*, *J. Phys. B* **28**, 591 (1995); T. Orlikowski, *Eur. Phys. J. D* **28**, 187 (2004).
- [30] M. Takamoto *et al.*, *Nature (London)* **435**, 321 (2005).